

Photochemical and structural properties of the cyclodextrin inclusion complexes of aryl-olefin bichromophores

Sandra Monti^{a,*}, Francesco Manoli^a, Ilse Manet^a, Giancarlo Marconi^a,
Bernd Mayer^b, Rosa E. Tormos^c, Miguel A. Miranda^c

^a *Istituto per la Sintesi Organica e la Fotoreattività (ISOF), Consiglio Nazionale delle Ricerche, Via Piero Gobetti 101, I-40129 Bologna, Italy*

^b *Emergentec Bioresearch, Rathausstrasse 5/3, A-1010 Vienna, Austria*

^c *Departamento de Química/Instituto de Tecnología Química UPV-CSIC, Universidad Politécnica de Valencia, UPV-CSIC, E-46022 Valencia, Spain*

Available online 17 May 2005

Abstract

The photoproducts distribution of 2-allylphenol (**1**), 2-allylanisole (**2**) and 2-allylaniline (**3**) were strongly modified by inclusion of these compounds in cyclodextrin (CD) cavities. Under these conditions photocyclization for **1** and **3** and di- π -methane photorearrangement for **2**, occurring in homogeneous solvents, were strongly depressed and photohydration of the acyclic olefin moiety was found to be by far the predominating photoprocess. The determination of the stability constants, the absorption properties, the steady state and time resolved fluorescence, the induced circular dichroism, accompanied by conformational calculations, of the CD complexes of **1–3**, allowed a rationale to be reached for the modified photochemical behavior of these compounds within the CD cavity, based on the structure of the 1:1 host–guest ground state complexes and on the influence of the intracavity interactions on the reactive singlet excited state of **1–3**.

© 2005 Elsevier B.V. All rights reserved.

Keywords: 2-Allylphenol; 2-Allylanisole; 2-Allylaniline; Cyclodextrin; Photochemistry

1. Introduction

The photoreactivity of organic guests in cyclodextrin (CD) inclusion complexes may be strongly modified by the decreased polarity, enhanced steric constraints or specific interactions provided by the CD environment [1,2]. A remarkable example of this effect can be found in the photochemistry of the non conjugated aryl-olefin bichromophoric compounds 2-allylphenol, 2-allylanisole, 2-allylaniline (**1–3** in Chart 1).

UV irradiation of these molecules in homogeneous solvents induces photocyclization to 5-membered ring products **4** (starting from **1** and **3**) and di- π -methane photorearrangement to product **5** (starting from **2**). These reactions are known to take place in the singlet manifold, via intramolecular pathways. The occurrence of intramolecular proton transfer in phenol derivatives [3–5] and electron transfer in aniline derivatives [6] was evidenced. The presence of a ground state XH- π interaction and the formation of intramolecular exci-

plexes were indicated to accompany photoreactivity [4–6]. The length of the linking chain as well as the presence of substituents on the chain itself, were also shown to be determining [3,4].

A preliminary communication reported that the addition of α -, β - and γ -CD (Chart 2) to the reaction medium drastically modified the photochemistry of **1–3** [7]. Under these conditions photocyclization of **1** and **3** and photorearrangement of **2** were strongly depressed and photohydration of the acyclic olefin moiety to give products **6** was found to be by far the predominating photoprocess [7]. This suggested us to reconsider the modified photochemical behavior of these bichromophoric guests in the light of the spectroscopic, photophysical and structural properties of their CD inclusion complexes.

The formation and the structure of the complexes were investigated by induced circular dichroism spectroscopy (icd) and conformational calculations using an ensemble of techniques, which afforded excellent results in determining the geometry of a variety of other cyclodextrin complexes [8–15]. They were based on a Dynamic Monte Carlo (DMC)

* Corresponding author. Tel.: +39 051 639 9813; fax: +39 051 639 9844.
E-mail address: monti@isof.cnr.it (S. Monti).

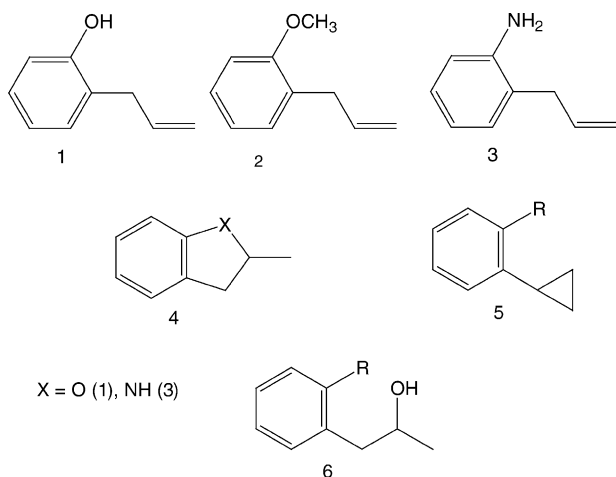


Chart 1. Structures of 2-allylaromatics and photoproducts.

approach, which included solvation effects and on icd calculations by quantum mechanical methods. The excited singlet photophysical properties were investigated by steady state and time resolved fluorescence. The results allowed a rationale to be formulated for the modified photoreactivity of compounds **1–3** in the CD cavity.

2. Experimental

2.1. Materials and methods

Compound **1** was commercially available. Treatment of **1** with methyl iodide afforded **2**. Compound **3** was obtained by Claisen rearrangement of *N*-allylaniline in presence of $ZnCl_2$, as described in the literature [6]. Cyclodextrins were from Serva. Acetonitrile and *n*-hexane were products of spectroscopic grade from Carlo Erba. Water was purified by a Millipore MilliQ system.

Irradiations of aerated solutions of **1–3** were performed using the quartz-filtered light of a 125 W medium pressure mercury lamp for 1 h. Parallel experiments were carried out in hexane or acetonitrile (5 mM) solution and in cyclodextrin/water (1.5 mM **1–3** and 7 mM CD). The photoproducts were identified comparing the MS spectra and the GC retention times with those of authentic samples and quantitated by GC using adequate standards.

Ultraviolet absorption spectra were recorded on a Perkin-Elmer $\lambda 9$ or a $\lambda 45$ spectrophotometer. Circular dichroism

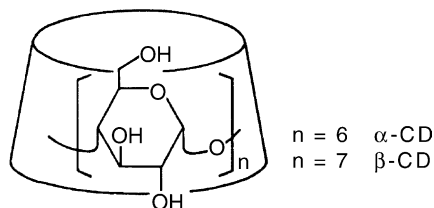


Chart 2. Cyclodextrin structures.

spectra were obtained with a Jasco J-710 dichrograph. Absorption and icd experiments were carried out in cells of 1 cm pathlength.

Fluorescence emission spectra were measured on a Spex Fluorolog 111A spectrofluorimeter. Right angle detection geometry was used. Experiments were carried out in cells of 1 cm pathlength with samples of absorbance <0.1 at the excitation wavelength. Fluorescence emission in titration experiments was obtained by exciting at isosbestic points. For emission quantum yield measurements naphthalene in cyclohexane was used as standard ($\Phi_f = 0.23$ in degassed solution reduced to 0.036 in air equilibrated solution) [16]. The low solubility of oxygen in water, the short fluorescence lifetimes (see below) and the protective action of the CD cage, cause the presence of oxygen to negligibly affect the emission intensity. Therefore air-equilibrated solutions both for the samples and the reference were used. For the CD complexes the emission quantum yields were evaluated from the ratio between the integrals of the emission spectra of the pure free and complexed species extracted by the global analysis method described below.

The best complexation model, the association constants and the pure spectra of the complexes were determined by global analysis of multiwavelength data of UV absorption, icd and fluorescence of the allylaromatics titrated with CD (typically 10 concentrations). The commercially available SPEC-FIT/32 (Spectrum Software Associates) computer program was used for this purpose.

Fluorescence lifetimes were determined by a time-correlated single photon counting system (IBH Consultants Ltd.), also on air-equilibrated solutions. The nanosecond flashlamp, filled with deuterium, was thyratron-driven at 40 kHz; the instrumental response function had a full width at half maximum of 2 ns. The absorbance of the solutions was ca. 0.2 in a 1 cm cell at the excitation wavelength (usually chosen in the 270–295 nm range). Emission was collected at 90° . Fluorescence decays were described by exponential functions and deconvolution of the instrumental response was performed by means of a non linear best fitting procedure using the least-squares method. The software package was provided by IBH Consultants Ltd. The resolution limit with deconvolution was ~ 0.3 ns.

All the spectroscopic and time resolved measurements were performed at 295 K.

2.2. Calculations

The conformation of the β -CD complexes of **1–3** was investigated by molecular mechanics using the MM3 Force Field to determine the coarse minima of potential energy along the complexation pathway. Dynamic Monte Carlo (DMC) annealing allowed the positions around the coarse minima to be explored by varying stochastically the relative orientation of host and guest. The solvent effect was included using a continuum model. Full reoptimization was performed at the geometries selected using the difference between the

Table 1
Photochemistry of Compounds 1–3

Entry	Substrate	Conditions ^a	Conversion	Product yield (%) ^b		
				4	5	6
1	1	A	22	100	–	–
2	1	B	34	80	20	–
3	1	C	95	–	31 ^b	69
4	1	D	85	13	44 ^b	43
5	2	A	55	–	100	–
6	2	B	42	–	100	–
7	2	C	58	–	63 ^b	37
8	3	A	54	100 ^c	–	–
9	3	B	57	100 ^c	–	–
10	3	C	94	45 ^c	–	–

^a A: Hexane, B: acetonitrile, C: β -CD/water, D: α -CD/water.

^b It includes the secondary products derived from 5 via hydrolytic ring opening.

^c It includes the indoline oxidation products (e.g. indole).

calculated icd and the experimental signal as a final test of the reliability of the geometries obtained from the DMC calculation [see refs.8–15]. The icd was calculated following the Tinoco–Kirkwood approach [17], a simplified version of the original dipole–dipole interaction term obtained introducing the polarizability of the macrocyclic bonds. According to this approximation, the equations of the rotational strength for a transition $0 \rightarrow a$ are given by

$$R_{0a} = \pi v_a \mu_{0a}^2 \sum_j \frac{v_{0j}^2 (\alpha_{33} - \alpha_{11})_j (GF)_j}{c(v_{0j}^2 - v_a^2)} \quad (1)$$

$$(GF)_j = \frac{1}{r_j^3} \left[\mathbf{e}_{0a} \mathbf{e}_j - \frac{3(\mathbf{e}_{0a} r_j)(\mathbf{e}_j r_j)}{r_j^2} \right] \mathbf{e}_{0a} \times \mathbf{e}_j r_j \quad (2)$$

where \mathbf{e}_{0a} and \mathbf{e}_j are unit vectors along the transition moment μ_{0a} and parallel to the j -th bond, respectively; v_{0j} and v_a are the frequencies of the electric transitions of the host and the guest, that are located at a distance r_j , and α_{11} , α_{33} represent the bond polarizabilities at zero frequency, parallel and perpendicular to the symmetry axis of the bond j -th. The equilibrium properties of the excited states of the guests were determined using the ZINDO/S program, with the Mataga–Nishimoto formulation for the Coulomb integrals. This method proved to be sensitive to reproduce the experimental icd spectra of several chromophores included in cyclodextrins. Details on the computational procedure adopted are fully reported in refs. [8–15].

3. Results and discussion

3.1. Photochemistry

Irradiation of 1 in hexane led to dihydrobenzofuran (4) as the only product (Table 1, entry 1).¹ In acetonitrile (Table 1,

entry 2), a mixture (4/1) of 4 and the cyclopropane (5) was obtained. It is known that 4 forms via intramolecular excited state proton transfer [18,19], while 5 is the di- π -methane photorearrangement product [20]. Photolysis of 1 in β -CD/water resulted in a much higher conversion, together with a dramatic change in the product distribution (Table 1, entry 3). In this case, cyclization to 4 was totally suppressed, to the benefit of alcohol 6. When α -CD was used (Table 1, entry 4) the hydration product yield was lower than with β -CD. Irradiation of 2 in hexane and acetonitrile (Table 1, entries 5 and 6) afforded 5 as the only product. By contrast, in cyclodextrin media (Table 1, entry 7) significant amounts of 6 were obtained. These results indicate that in solution the di- π -methane photorearrangement is the only occurring process, while inside CD it has to compete with photohydration.

As allylanilines undergo intramolecular electron transfer (rather than proton transfer) in their excited states [21], *o*-allylaniline 3 was selected as a probe to check whether this type of process also contributes to enhance photohydration. In agreement with previous observations [21], direct photolysis of 3 in hexane (Table 1, entry 8) afforded indoline 4, together with indole as secondary oxidation product. In acetonitrile (Table 1, entry 9), the same products were obtained. However, when photolysis of 3 was carried out in β -CD/water alcohol 6 was the major product. Lower amounts of 4 and indole were also obtained. These results indicate that intramolecular excited state electron transfer also contributes to photohydration, although to a lesser extent than proton transfer.

3.2. Spectroscopy and photophysics

3.2.1. Allylphenol and allylanisole

The absorption spectrum of 1 in water exhibited a band peaked at 271 nm with a red-side shoulder at 278 nm and a more intense band peaked below 220 nm. In presence of α -CD or β -CD a red shift of the lowest energy band by ca. 2–3 nm was observed (Fig. 1).

¹ Other minor products have been previously identified upon irradiation of 1 for longer irradiation times. See M.A. Miranda and R. Tormos, J. Org. Chem. 58 (1993) 3304.

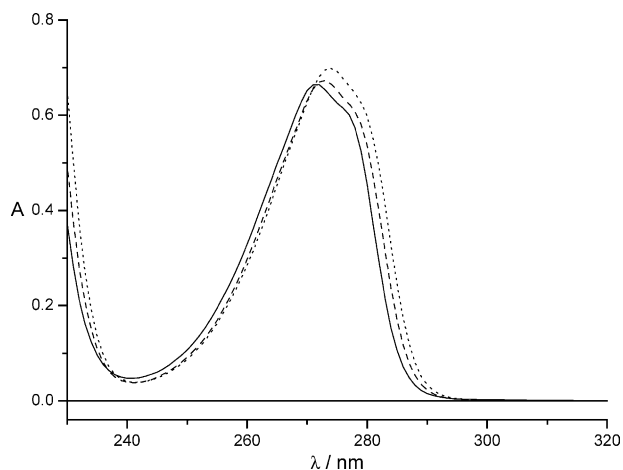


Fig. 1. Absorption spectra of 2-allylphenol 1.8×10^{-3} M in water (solid), in presence of 3×10^{-2} M α -CD (dash), in presence of 1.3×10^{-2} M β -CD (dot). Cell 0.2 cm.

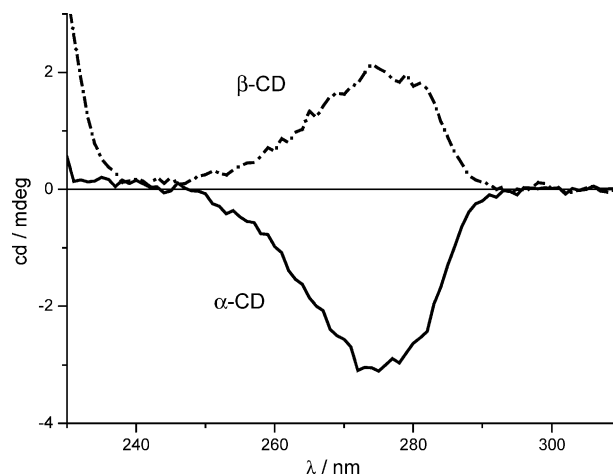


Fig. 2. icd of 2-allylphenol 1.8×10^{-3} M in presence of 3×10^{-2} M α -CD (solid) and of 1.3×10^{-2} M β -CD (dashed-dot). Cell 0.2 cm.

The induced circular dichroism signal was negative with α -CD and positive with β -CD (Fig. 2). UV absorption and icd variations were used (by titrating **1** with α -CD in the $0\text{--}5 \times 10^{-2}$ M range and with β -CD in the $0\text{--}1.5 \times 10^{-2}$ M range) to assess the best complexation model. A 1:1 stoichiometry, the molar absorption coefficients and the equilibrium constants for the inclusion complexes were determined (Table 2).

The fluorescence of **1** in water was characterized by an unstructured band peaked at 300 nm with $\Phi_f = 0.072$ in air equilibrated solution. The emission intensity was enhanced by addition of α - and β -CD without change of the spectral profile (see for example Fig. 3). The analysis of the inten-

sity changes upon excitation at the isosbestic point of the absorption variations confirmed 1:1 stoichiometry and association constants values, determined by UV absorption and icd. The emission quantum yields of the α - and β -CD complexes indicated a substantial increase of the fluorescence capability for the included vs. the free guest (Table 2).

Fluorescence lifetimes were measured by exciting a 1.2×10^{-4} M solution of **1** in water at 274 nm and detecting the emission at 310 nm. Good monoexponential decay with 2.0 ns lifetime ($\chi^2 = 1.1$) was evidenced. By addition of 1×10^{-2} M β -CD, the decay exhibited two components with lifetimes $\tau_1 = 1.7$ ns and $\tau_2 = 3.9$ ns and relative amplitudes 29

Table 2

Spectroscopic, photophysical and equilibrium parameters of aryl olefins **1–3** and their α - and β -CD inclusion complexes, determined at 295 K

	1	2	3
$\epsilon_{\text{free}}^{\text{max}}$ ($\text{M}^{-1} \text{cm}^{-1}$)	1900	1400	1830
λ_{max} (UVabs)	271 nm	271 nm	282 nm
$\Phi_{\text{free}}^{\text{a}}$	0.072 ^b	0.11 ^b	0.007–0.013 ^d
$\tau_{\text{free}}/\text{ns}^{\text{a}}$	2.0 ($\lambda_{\text{em}} = 310 \text{ nm}$) ^b	3.9 ($\lambda_{\text{em}} = 310 \text{ nm}$) ^b	$\leq 0.3, 0.32, 6.1$ ($\lambda_{\text{em}} = 325 \text{ nm}$) ^g , ($\lambda_{\text{em}} = 410 \text{ nm}$) ^g
$\log K_{\text{ass}}^{\alpha}$ (M^{-1})	2.31 (UVabs) ^c , 2.39 (FL) ^c	2.36 (UVabs, icd)	2.18 (FL) ^e
Φ_{α}^{a}	0.12 ^b	0.11 ^b	0.03 ^f
$\tau_{\alpha}/\text{ns}^{\text{a}}$	3.6	5–6	0.6, 5.6 ($\lambda_{\text{em}} = 340 \text{ nm}$) ^f
$\epsilon_{\alpha}^{\text{max}}$ ($\text{M}^{-1} \text{cm}^{-1}$)	2000	1600	1600
λ_{max} (UVabs)	273 nm	271 nm	283 nm
$\Delta\epsilon_{\alpha}$ ($\text{M}^{-1} \text{cm}^{-1}$)	−0.31	−3.2	−0.22
$\log K_{\text{ass}}^{\beta}$ (M^{-1})	2.52 (UVabs) ^c , 2.64 (FL) ^c , 2.46 (icd) ^c	2.8 (FL)	2.18 (FL) ^e
Φ_{β}^{a}	0.11	0.14	0.02 ^g
$\tau_{\beta}/\text{ns}^{\text{a}}$	3.9	5–6	0.5, 4.6 ($\lambda_{\text{em}} = 325 \text{ nm}$) ^g , 0.6, 6.4 ($\lambda_{\text{em}} = 410 \text{ nm}$) ^g
$\epsilon_{\beta}^{\text{max}}$ ($\text{M}^{-1} \text{cm}^{-1}$)	1900	1250	1750
λ_{max} (UVabs)	274 nm	272 nm	283 nm
$\Delta\epsilon_{\beta}$ ($\text{M}^{-1} \text{cm}^{-1}$)	+0.23	+0.02	−0.06

^a Air equilibrated solutions, uncertainty $\pm 10\%$

^b $\lambda_{\text{exc}} = 272 \text{ nm}$.

^c Error on $\log K_{\text{ass}} < 0.025$.

^d Total quantum yield at $\lambda_{\text{exc}} = 284$ and 292 nm , respectively.

^e Error on $\log K_{\text{ass}} < 0.04$.

^f $\lambda_{\text{exc}} = 292 \text{ nm}$.

^g $\lambda_{\text{exc}} = 284 \text{ nm}$.

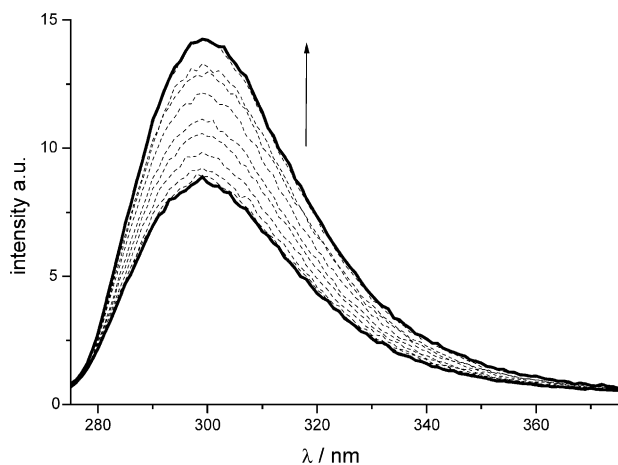


Fig. 3. Emission intensity of 2-allylphenol 5.4×10^{-5} M as a function of the α -CD concentration in the range $0\text{--}3 \times 10^{-2}$ M; $\lambda_{\text{exc}} = 272$ nm.

and 71%, respectively ($\chi^2 = 1.1$).² No equilibration between free and complexed molecules was expected during the short lifetime of the excited state, so that the two components were assigned to the fractions relevant to the ground state equilibrium. Similar results were obtained with 3×10^{-2} M α -CD.

The values of the association constants of allylphenol to α -CD and β -CD are in the order of those generally found for substituted phenol derivatives [22]. The photophysical parameters of the inclusion complexes (increase of the fluorescence quantum yield accompanied by lengthening of the emission lifetime), indicate halving of the rate constant for non radiative deactivation, k_{nr} , of the guest in the cavity with respect to bulk solvent, and substantial constancy (within 20%) of the radiative rate parameter (see Eqs. (3) and (4)).

$$k_r = \frac{\Phi_f}{\tau} \quad (3)$$

$$k_{\text{nr}} = (1/\tau) - k_r \quad (4)$$

Analogous investigation was performed of the interaction of 2-allylanisole (2) with α - and β -CD. Formation of 1:1 complexes was assessed on the basis of UV absorption, icd and fluorescence data (Figs. 4 and 5, Table 2).³ The icd in presence of β -CD was positive but, being very weak, was not useful to determine K_{ass} .

The emission in water was characterized by a unstructured band peaked at 296 nm ($\Phi_f = 0.11$ in air equilibrated solution). Titration with CDs ($\lambda_{\text{exc}} = 279$ nm) caused a slight enhancement of the intensity, which allowed the association

² Relative amplitude of the i component corresponds to $A_i \tau_i / \sum_j A_j \tau_j$ with A_i preexponential factor.

³ The scarce solubility in water of this oily substance caused some troubles due to precipitation during long lasting experiments of titration with CDs. This problem was controlled by keeping as low as possible the concentration of 2-allylanisole in the mother solution ($\sim 5\text{--}6 \times 10^{-4}$ M) and by repeating several times the same experiment with different modes of operations (dissolution of CD powder or dilution/mixing with CD solutions, variation of the sequential order of titrant concentrations).

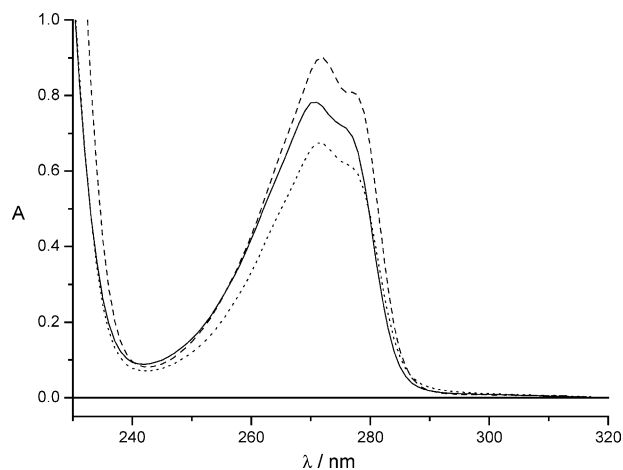


Fig. 4. Absorption spectra of 2-allylanisole 5.2×10^{-4} M in water (solid), in presence of 5×10^{-2} M α -CD (dash), in presence of 1.0×10^{-2} M β -CD (dot). Cell 1.0 cm.

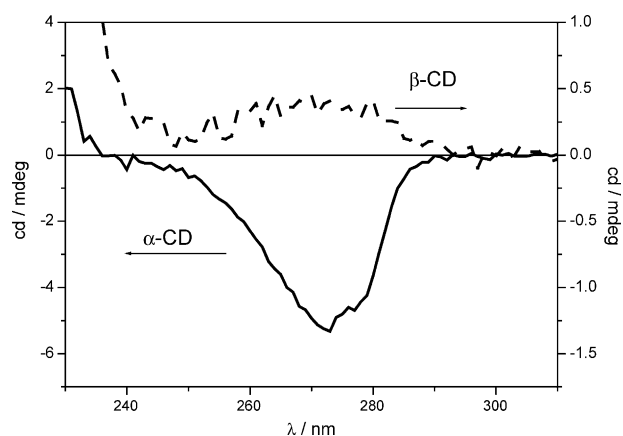


Fig. 5. ICD of 2-allylanisole 5.2×10^{-4} M in presence of 5×10^{-2} M α -CD (solid) and of 1.0×10^{-2} M β -CD (dash). Cell 1.0 cm.

constants of the 1:1 complexes to be obtained. The quantum yields were found to be similar in the free and the complexed molecule (Table 2).⁴

Time resolved experiments ($\lambda_{\text{exc}} = 272$ nm and $\lambda_{\text{em}} = 310$ nm) evidenced a single species with 3.9 ns lifetime ($\chi^2 = 1.0$) in pure water. Upon addition of 3×10^{-2} M α -CD the decay could still be described by a monoexponential function with lifetime of 4.6 ns ($\chi^2 = 1.2$). In presence of 1×10^{-2} M β -CD biexponential analysis was performed by fixing τ_1 at 3.9 ns for the free component. A second component with $\tau_2 = 5.9$ ns ($\chi^2 = 1.5$) was evidenced. Triexponential analysis did not provide better results. It was concluded that inclusion in CDs led to lengthening of the lifetime from 3.9 ns to ca. 5–6 ns but the contributions of the free and complexed species could not be rigorously separated. Too close lifetime values and possible presence of more than one complexation mode can be hypothesized to be responsible for such a behavior.

⁴ The emission enhancements were corrected to take into account that the excitation at $\lambda_{\text{exc}} = 279$ nm is not strictly isosbestic in the absorption spectra.

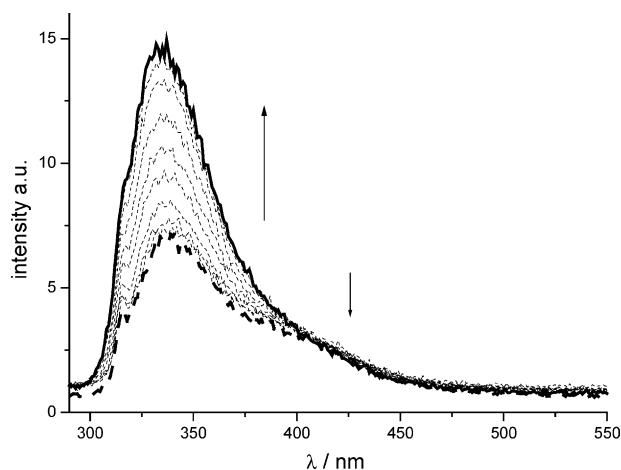


Fig. 6. Emission intensity of 2-allylaniline 5.0×10^{-5} M as a function of the β -CD concentration in the range $0\text{--}1.3 \times 10^{-2}$ M; $\lambda_{\text{exc}} = 284$ nm.

Despite the association constants for allylanisole are comparable to those for allylphenol, the inclusion has no effect on the photophysical parameters in the case of α -CD and induces only ca 25% decrease of k_{nr} in the case of β -CD.

3.2.2. Allylaniline

The absorption spectrum of 1.2×10^{-3} M 2-allylaniline (**3**) in water exhibited a maximum at 282 nm and a more intense band peaked at 230 nm. With $\lambda_{\text{exc}} = 284$ nm the fluorescence spectrum is characterized by a band peaked at ca. 335 nm and a shoulder at ca. 380–400 nm (Fig. 6). The shoulder became a well distinct band peaked at 400 nm by excitation at 292 nm (Fig. 7). The excitation spectrum of the emission at 330 nm had a maximum at ca. 282 nm, well corresponding to the maximum of the absorption spectrum, whereas the excitation spectrum of the emission at 400 nm had a maximum at ca. 300 nm. Saturation of the solution with oxygen lowered

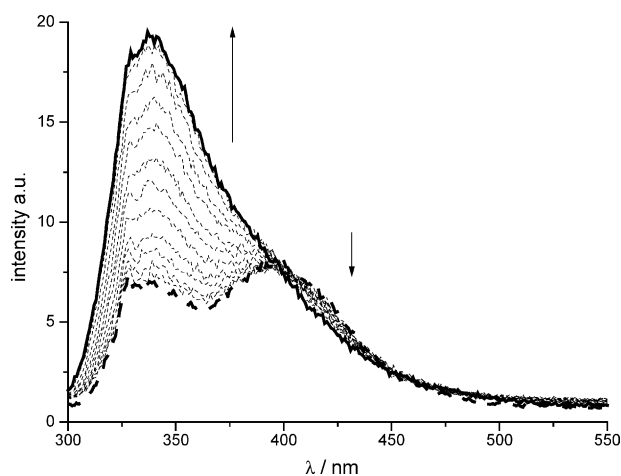


Fig. 7. Emission intensity of 2-allylaniline 1.2×10^{-4} M as a function of the α -CD concentration in the range $0\text{--}5 \times 10^{-2}$ M; $\lambda_{\text{exc}} = 292$ nm.

the intensity of the emission shoulder at 380–400 nm more than the intensity of the band at 335 nm.

A reasonable explanation of the above findings is the presence in solution of two emitting species. Because of the high quality of the **3** sample, we excluded the presence of an impurity in the original product. However we considered the possibility that some photodegradation of the solute occurred in the manipulation of the samples. Therefore the fluorescence spectra of the main photoproducts of **3** in water, 2-methyl-indoline and 2-methylindole [6] were checked. Both peaked in the 340–360 nm region and not at 400 nm, so that it was concluded that such photoproducts were not involved. Analogous long-wavelength emission band was assigned in allylquinolines to a ground state NH/ π complex [23]. On this basis the presence of dual emission in **3** could be reasonably attributed to the formation of a similar species. In order to check this hypothesis, the absorption spectra of **3** were recorded at different concentrations and compared with those of *o*-toluidine, the reference compound lacking the allyl substituent, at the same concentrations. Acetonitrile was used as solvent to improve solubility. The difference spectra, reported in Fig. 8 clearly show a well-defined emerging band with maximum at 307 nm, well corresponding to the maximum of the excitation spectrum of the long-wavelength emission in acetonitrile. This result indicates that both the NH group and the olefin are necessary for the formation of this species, which is therefore definitely assigned to an intramolecular folded conformation of **3**, in equilibrium with the “open” ones, in the ground state.

Addition of α - or β -CD induced a small red shift (ca. 1 nm) in the absorption spectrum of **3**, appearance of negative icd signals (Fig. 9) and variations in the emission (shape and intensity) with the band peaked at 335 nm strongly enhanced and that at 380–400 nm diminished. The intensity changes were interpreted by assuming the following model,

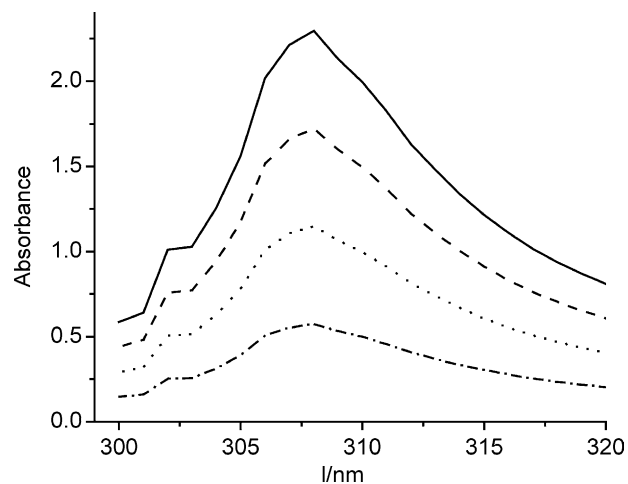


Fig. 8. Difference absorption spectra in the long wavelength region between equimolar 2-allylaniline and *o*-toluidine solutions in acetonitrile: 4×10^{-3} M (solid), 3×10^{-3} M (dash), 2×10^{-3} M (dot), 1×10^{-3} M (dash-dot). Cell 1.0 cm.

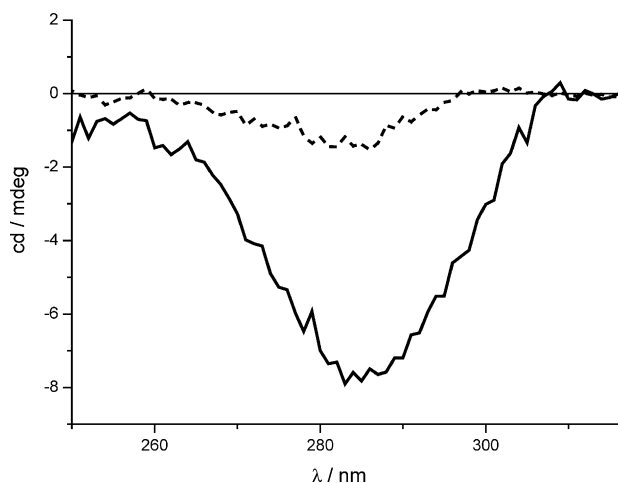


Fig. 9. icd of 2-allylaniline 1.2×10^{-3} M in presence of 5×10^{-2} M α -CD (solid) and of 1.0×10^{-2} M β -CD (dash). Cell 1.0 cm.

which resulted to be enough for a reliable global analysis of the data: emission from free and CD-complexed species with molar fractions relevant to the ground state equilibrium, interconversion of guest conformations faster than CD in-

clusion, formation of a single CD complex with 1:1 stoichiometry. Association constants extracted are reported in Table 2.

The total emission quantum yield (from all the conformations) in water, 0.007 and 0.013 for $\lambda_{\text{exc}} = 284$ and 292 nm, respectively, increased to 0.02 in the β -CD complex ($\lambda_{\text{exc}} = 284$ nm, isosbestic) and to 0.03 in the α -CD complex ($\lambda_{\text{exc}} = 292$ nm, isosbestic).

Lifetimes were measured for excitation at 284 nm. In water the fluorescence decay at 325 nm, analyzed with a monoexponential function, gave a lifetime below the instrumental resolution (<0.3 ns) and bad χ^2 . Biexponential analysis did not provide better results. In the case of the 410 nm emission biexponential analysis ($\chi^2 = 1.0$) gave two lifetimes of 0.32 ns (rel. ampl. 10%) and 6.1 ns (rel. ampl. 90%). By addition of 1×10^{-2} M β -CD, the decay at 325 nm became biexponential ($\chi^2 = 1.2$) with lifetimes of 0.5 ns (96%) and 4.6 ns (4%). The decay at 410 nm remained biexponential ($\chi^2 = 1.0$) with 0.6 ns (16%) and 6.4 ns (84%) lifetimes. The results with α -CD were similar (see Table 2).

On the basis of the steady state and time resolved emission data it was reasonably concluded that the emission component predominant at 320–330 nm, with a lifetime below

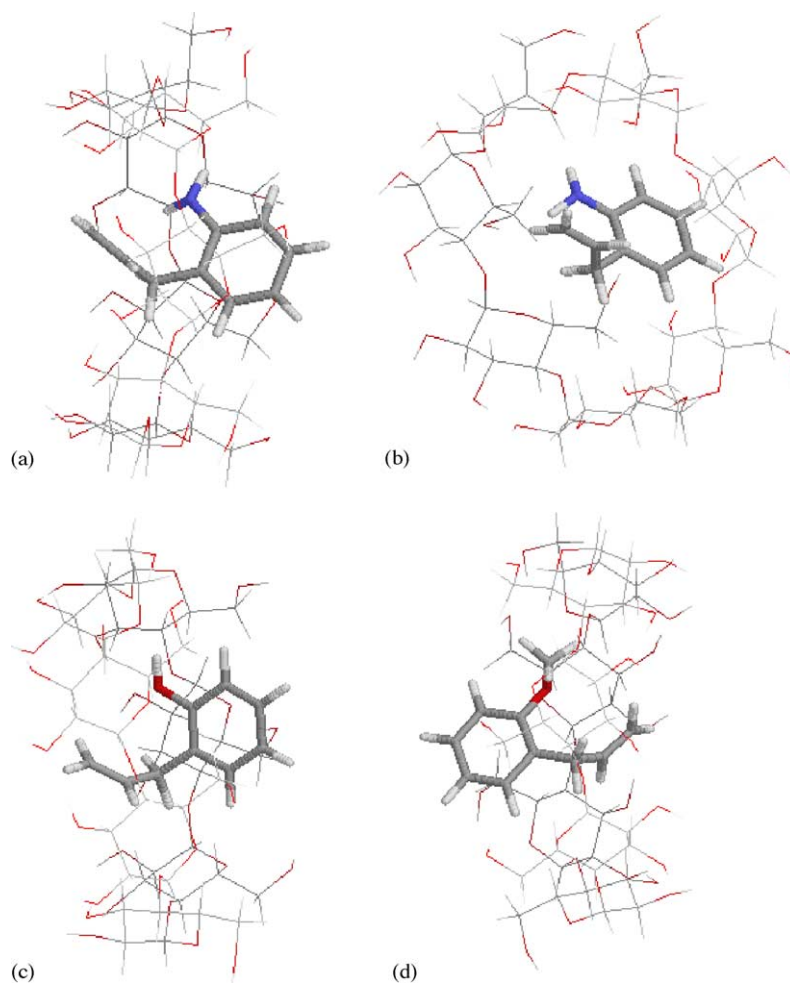


Fig. 10. Calculated structure of the 1:1 β -CD-aryl-olefin inclusion complexes: a and b, 2-allylaniline; c, 2-allylphenol; d, 2-allylanisole.

Table 3

Calculated energies (eV), oscillator strengths (f), rotational strengths (R_0 , 10^{-40} cgs) of the lowest singlet states of the examined β -CD complexes and complexation energy (kcal/mol) of their most stable conformation

1	2	3
S_1 , 4.59; f , 0.03; R_0 , 0.19	S_1 , 4.55; f , 0.02; R_0 , 0.30	S_1 , 4.52; f , 0.04; R_0 , -0.42
S_2 4.91; f 0.02; R_0 0.26	S_2 , 4.86; f , 0.03; R_0 , 0.24	S_2 , 4.80; f , 0.03; R_0 , -0.25
ΔE_c , -10.82	ΔE_c , -6.56	ΔE_c , -9.96

the instrumental resolution, was likely due to the excitation of “open” conformation(s) of **3** which became longer lived (0.5–0.6 ns) upon CD inclusion; on the other hand the emission at 400–420 nm with lifetime of 5–6 ns, unaffected by the CD, and with decreased relative amplitude in presence of CD, corresponded to excitation of folded conformation, which did not include appreciably. Consistently the relevant steady state emission intensity was slightly depressed (Figs. 6 and 7).

3.2.3. Conformation of the β -CD complexes

The scanning of 1000 possible conformations in the DMC docking process gave rise to a selection of 665, 746 and 711 complexes of β -CD and **1**, **2** and **3**, with the most stable structures evaluated at 56.24, 65.76 and 67.27 Kcal/mol, respectively (the sum of the energy of the separated molecules was 67.06, 72.32 and 77.23 kcal/mol). It was found that the last 100 most stable complexes for the three compounds satisfied the icd criterion, giving rise to a positive band for **1** and **2** and to a negative one for **3** in the region of the first absorption band (see Figs. 2, 5 and 9). The surface scanned during the DMC procedure appears flat, in line with the large degree of freedom characterizing the motions of the allyl, hydroxy, methoxy and amino substituents. The most stable structures so found are shown in Fig. 10, whereas the corresponding calculated transition energies and rotational strengths for the two lowest energy singlets, both involved in the lowest energy absorption band, are displayed in Table 3. The weak calculated icd is in reasonable agreement with the small experimental $\Delta\varepsilon$ values (see Figs. 2, 5 and 9 and Table 2).

All the compounds examined appear deeply embedded in the CD cavity, with the aromatic moiety partly exposed on the side of the primary rim. It is interesting to notice that the compounds are hosted in the CD cavity with a quite “open” structure as regards the aryl substituents and the allylic group: for example for **3** the distance between the allylic carbons C_1 and C_2 atoms and the amino nitrogen are calculated as $N-C_1 = 3.567 \text{ \AA}$ and $N-C_2 = 3.357 \text{ \AA}$.

4. Conclusions

In the CD cavity photocyclization of **1** and **3** and photorearrangement of **2** were strongly depressed in favour of photohydration of the acyclic olefin moiety. Such a change in the photochemical pattern can be related to the structural features of the ground state complexes as determined by icd

and computational studies of the β -CD systems. Actually no significant differences were observed between α - and β -CD in the photochemical behavior, the association constants and the spectroscopic and photophysical properties of the inclusion complexes of compounds **1–3**.

These molecules appear to be accommodated in the CD cavity in a quite extended conformation which reasonably disfavours, with such a constrained microenvironment, folding to a geometry suitable for ring closure. Actually OH- π interactions have been shown to play a key role in the cyclization of allylphenol derivatives [3].

In the allylaniline system a “closed” conformation was experimentally observed in homogeneous solvents owing to its red-shifted fluorescence. The presence of charge-transfer induced emissions in allylazaaromatics has been associated to the occurrence of photocyclization. Consistently, a previous PCILO conformational study on both the ground and the excited state of *N*-methyl *o*-2-butenylaniline showed that the lowest energy conformation is a folded structure in which excitation transfer from the excited aniline chromophore to a twisted singlet zwitterionic excited state makes possible photochemical closure [24]. According to this picture, in the CD cavities, where cyclization is disfavoured, efficient inclusion of such “closed” conformations of **3** does not occur, the conformational equilibrium being shifted by the inclusion toward “open” structures.

The photophysical parameters of the excited singlet state of **1** and **2** (known to be the photochemically active one) indicate a specific influence of the cavity interactions on the deactivation pathways. Decrease of the overall non radiative rate constant, manifested in the lengthening of the lifetime, is indeed consistent with a substantial steric hindrance reducing the molecular degrees of freedom of the guest, which assist the conversion of electronic energy either into lower energy vibrational modes or into the intramolecular photochemical channels.

Finally, lowering of the environmental polarity reasonably also plays a role. Indeed it tends to disfavour excited state intramolecular proton transfer (for **1**) or electron transfer (for **3**), which promote photocyclization reactions via zwitterionic intermediates. Moreover, in the case of **2**, it is expected to destabilize species, which have been postulated as intermediates in di- π -methane photorearrangement [25].

All this considered, a bimolecular attack by a water molecule in close proximity of the CD rim (or included in the cavity) either directly to the excited state

of **1–3** or to a subsequent intermediate could reasonably compete with the intramolecular processes of photocyclization/photorearrangement and lead to the formation of hydration products in high yields.

References

- [1] P. Bortolus, S. Monti, *Adv. Photochem.* 21 (1996) 1–133.
- [2] S. Monti, S. Sortino, *Chem. Soc. Rev.* 31 (2002) 287–300.
- [3] M. Teresa Bosch-MontalvÀ, L.R. Domingo, M. Consuelo Jimenez, M.A. Miranda, R. Tormos, *J. Chem. Soc. Perkin Trans. 2* (1998) 2175–2179.
- [4] M. Consuelo Jimenez, M.A. Miranda, R. Tormos, S. Gil, *Eur. J. Org. Chem.* (2002) 297–300.
- [5] F. Galindo, M. Consuelo Jimenez, M.A. Miranda, R. Tormos, *Chem. Commun.* (2000) 1747–1748.
- [6] O. Benali, M.A. Miranda, R. Tormos, *Eur. J. Org. Chem.* (2002) 2317–2322.
- [7] O. Benali, M. Consuelo Jimenez, M.A. Miranda, R. Tormos, *Chem. Commun.* (2001) 2328–2329.
- [8] H.-R. Park, B. Mayer, P. Wolschann, G. Köhler, *J. Phys. Chem.* 98 (1994) 6158–6166.
- [9] G. Grabner, S. Monti, G. Marconi, B. Mayer, Ch.Th. Klein, G. Köhler, *J. Phys. Chem.* 100 (1996) 20068–20075.
- [10] P. Bortolus, G. Marconi, S. Monti, B. Mayer, G. Köhler, G. Grabner, *Chem. Eur. J.* 6 (2000) 1578–1591.
- [11] P. Bortolus, G. Marconi, S. Monti, B. Mayer, *J. Phys. Chem. A* 106 (2002) 1686–1694.
- [12] S. Monti, G. Marconi, F. Manoli, P. Bortolus, B. Mayer, G. Grabner, G. Köhler, W. Boszczyk, K. Rotkiewicz, *Phys. Chem. Chem. Phys.* 5 (2003) 1019–1026.
- [13] S. Monti, P. Bortolus, F. Manoli, G. Marconi, G. Grabner, G. Köhler, B. Mayer, W. Boszczyk, K. Rotkiewicz, *Photochem. Photobiol. Sci.* 2 (2003) 203–211.
- [14] G. Marconi, S. Monti, F. Manoli, A. Degli Esposti, B. Mayer, *Chem. Phys. Lett.* 383 (2004) 566–571.
- [15] G. Marconi, S. Monti, F. Manoli, A. Degli Esposti, A. Guerrini, *Helv. Chim. Acta* 87 (2004) 2368–2377.
- [16] B. Berlman, *Handbook of Fluorescence Spectra of Aromatic Molecules*, Academic Press, New York, 1971, p. 330.
- [17] I. Tinoco Jr., *Adv. Chem. Phys.* 4 (1962) 113–160.
- [18] H. Fráter, Schmid, *Helv. Chim. Acta* 50 (1967) 255–262.
- [19] A. Shani, R. Mechoulam, *Tetrahedron* 27 (1971) 601–606.
- [20] T. Kitamura, T. Imagawa, M. Kawanisi, *Tetrahedron* 34 (1978) 3451–3457.
- [21] U. Koch-Pomeranz, H. Schmid, H.-J. Hansen, *Helv. Chim. Acta* 60 (1977) 768–797.
- [22] M.V. Rekharsky, Y. Inoue, *Chem. Rev.* 98 (1998) 1875–1917.
- [23] E. Leo, R. Tormos, S. Monti, L.R. Domingo, M.A. Miranda, *J. Phys. Chem A* 109 (2005) 1758–1763.
- [24] G. Trinquier, N. Paillous, A. Lattes, J.P. Malrieu, *Nouv. J. Chim.* 1 (1977) 403–411.
- [25] M. Consuelo Jimenez, M.A. Miranda, R. Tormos, *Chem. Commun.* (2000) 2341–2342.